

Measurement of air and nitrogen fluorescence light yields induced by electron beam for UHECR experiments

P. Colin ^{a d 1}, A. Chukanov ^b, V. Grebenyuk ^b, D. Naumov ^{b e},
 P. Nédélec ^a, Y. Nefedov ^b, A. Onofre ^c, S. Porokhovi ^b,
 B. Sabirov, ^b L. Tkatchev ^b

The MACFLY Collaboration:

^a*Laboratoire d'Annecy-le-Vieux de Physique des Particules, IN2P3/CNRS,
 Université de Savoie, Annecy-le-Vieux, FRANCE*

^b*Joint Institute for Nuclear Research
 Dubna, Moscow region, RUSSIA*

^c*Laboratorio de Instrumentação e Física Experimental de Partículas
 Coimbra, PORTUGAL*

^d*Department of Physics, University of Utah
 Salt-Lake-City, Utah, USA*

^e*Instituto Nazionale di Fisica Nucleare, Firenze, ITALY*

Abstract

Most of the Ultra High Energy Cosmic Ray (UHECR) experiments and projects (HiRes, AUGER, TA, EUSO, TUS,...) use air fluorescence to detect and measure extensive air showers (EAS). The precise knowledge of the Fluorescence Light Yield (FLY) is of paramount importance for the reconstruction of UHECR. The MACFLY - Measurement of Air Cherenkov and Fluorescence Light Yield - experiment has been designed to perform such FLY measurements. In this paper we will present the results of FLY in the 290-440 nm wavelength range for dry air and pure nitrogen, both excited by electrons with energy of 1.5 MeV, 20 GeV and 50 GeV. The experiment uses a ⁹⁰Sr radioactive source for low energy measurement and a CERN SPS e⁻ beam for high energy. We find that the FLY is proportional to the deposited energy (E_d) in the gas and we show that the air fluorescence properties remain constant independently of the electron energy. At the reference point: atmospheric dry air at 1013 hPa and 23°C, the ratio $FLY/E_d=17.6$ photon/MeV with a systematic error of 13.2%.

¹ contact address: colin@physics.utah.edu

1 Introduction

The physics of the Ultra High Energy Cosmic Rays (UHECR) is a challenging search in the field of cosmic ray physics. There is a special interest to measure the energy spectrum in the region of 10^{20} eV where the GZK cutoff is predicted (1). For more than 40 years, many experiments looked for such UHECR events but only a few dozen of them have been recorded so far. The lack of statistics and the discrepancies between the results of the two main experiments AGASA (2) and HIRES (3), requires new experiments to solve the UHECR and the GZK puzzle. In the coming years, with the deployment of ground based detectors: the Pierre Auger Observatory (4) and the Telescope Array (5), this number of events will increase dramatically, reaching several hundreds. In the longer term, space-based experiments (OWL, EUSO, TUS) (6) are foreseen, with the goal of reaching a thousand events per year.

For most of the past, present and future experiments, the detection technique relies, at least, on the measurement of the air fluorescence produced by the incoming cosmic ray showering in the atmosphere. This light, observed in the near-UV region, is induced by the de-excitation of the molecule of air (mainly N_2) occurring along the development of the extensive air showers (EAS). This Fluorescence Light Yield (FLY) is rather weak (~ 4 photons/m emitted in 4π), and depends significantly on the atmospheric conditions (temperature, pressure, gas components: H_2O , Ar, ...).

Since the 1960's, when it was first proposed to use air fluorescence for UHECR's detection, the FLY has been studied. In 1967, A. N. Bunner summarized the existing data in his thesis (7). At that time the uncertainty on the FLY was ~ 30 % ! Later, the discrepancy between the AGASA and HiRes experiments led the UHECR community to pursue their efforts on the FLY measurement. In 1996, in the context of HiRes and Telescope Array, a new set of results (8) was published. More recently, M. Nagano *et al.* released new measurements on the FLY with systematic uncertainty of ~ 13.2 % (9).

A better understanding of the FLY, with a goal of setting the systematic uncertainties below 10 %, is now needed for the UHECR experiments. Up to now only the pressure dependence was really measured. To improve our knowledge of air FLY and its behavior with respect to pressure, temperature, humidity, electron energy, shower age, etc, new experiments are needed. An overview of the current experiments can be found elsewhere (10).

This paper is organized as follows: Section 2 describes the fluorescence mechanisms and presents a predictive model. In Section 3 the experimental setup is described. In Section 4 the data taking and signal processing are discussed and in Section 5 the calibration and systematic studies are presented. Finally our

results are described in Section 6 and a comparison with other experiments are discussed in Section 7.

2 Air fluorescence mechanisms and production model

The Fluorescence Light Yield depends on two competitive processes: excitation and de-excitation of the air molecules.

In an EAS, the air is excited by the high energy charged particles of the shower. When such a particle traverses the air, it ionizes air and produces secondary low energy electrons which will excite N_2 molecules in the low energy states (10-20 eV), which fluoresce. The energy (and hence the wavelength) of the fluorescence photons corresponds to the energy difference between two excited states of an air molecule: the spectrum varies in a large band, from UV to IR. In the UHECR experiments, the photons are detected in the near UV band, which ranges in the 290-440 nm window in MACFLY.

A molecular excited state can be defined by its molecular orbital and by its vibrational state. The air fluorescence spectrum at atmospheric pressure is a band spectrum dominated by 1N system of N_2^+ and 2P system of N_2 . 1N system corresponds to all the transitions between N_2^+ orbitals $B^2\Sigma_u^+$ and $X^2\Sigma_g^+$, and 2P system to all the transitions between N_2 orbitals $C^3\Pi_u$ and $B^3\Pi_g$ (11).

During the de-excitation, there is a contest between the radiative and the non-radiative processes, which are both characterized by a time scale. The first one may produce photons in the experimental UV band while the second process dissipates the energy via thermal processes.

The mean lifetime τ_e of an excited state in non-isolated conditions verifies:

$$\frac{1}{\tau_e} = \frac{1}{\tau_{e0}} + \sum \frac{1}{\tau_{eC}^i}, \quad (1)$$

where the first term τ_{e0} is the mean lifetime of the isolated excited state. For instance the typical values of the 2P system are ~ 40 ns (12).

The non-radiative de-excitation of the molecules (quenching) comes from collisions of the excited molecules with other air molecules. The collision times τ_{eC}^i of the excited state e with the molecule of type i ($i = N_2, O_2, H_2O, \dots$) are given by the kinematic theory of gases:

$$\tau_{eC}^i = \frac{1}{Pi} \frac{\sqrt{\pi kT m_{N_2}}}{4\sigma_e^i} \sqrt{\frac{2m_i}{m_{N_2} + m_i}},$$

where T is the gas temperature, P^i is the partial pressure of molecules i , k is the Boltzmann constant, m_{N_2} and m_i are the molecular mass of N_2 and of molecule i , and σ_e^i is the cross section of the collision. The τ_{eC}^i have been measured since a long time and their values vary inversely with the pressure P . At atmospheric pressure the quenching time of the 2P system is a few ns.

One often expresses the relationship between the lifetime and the pressure via the formula:

$$\frac{1}{\tau_e} = \frac{1}{\tau_{e0}} \left(1 + \frac{P}{P'}\right), \quad (2)$$

P' being the pressure for which the quenching processes have a collision time equal to the radiative de-excitations lifetime.

In our model, the quenching processes are characterized by the quenching factors k_e^i , independent of the pressure, defined by: $k_e^i = \frac{4\sigma_e^i}{\sqrt{\pi k T m_{N_2}}} \sqrt{\frac{m_{N_2} + m_i}{2m_i}}$.

Assuming that σ_e^i do not vary with temperature, implies that the k_e^i vary solely as the inverse square root of the temperature: $k_e^i(T) = k_e^i(T_0) \sqrt{\frac{T_0}{T}}$. The values of $k_e^i(T_0)$ are given for a reference temperature T_0 .

Thus, τ_{eC}^i can be re-written as:

$$\tau_{eC}^i(P, T) = \frac{1}{P \times f^i \times k_e^i(T)}. \quad (3)$$

For any excited states, e , of a gas at temperature T and pressure P containing a fraction f^i of molecules i , the probability \mathcal{Q} to have a radiative de-excitation is:

$$\mathcal{Q} = \frac{1}{\tau_{e0}} / \frac{1}{\tau_e} = \frac{\tau_e}{\tau_{e0}} = \frac{1}{1 + P \tau_{e0} \sum f^i k_e^i(T_0) \sqrt{\frac{T_0}{T}}}.$$

For all the air fluorescence lines, at wavelength λ , corresponding to an excited state e , one can express the $\frac{FLY}{E_d} \Big|_{\lambda}$ ratio of an arbitrary admixture of N_2 , O_2 and H_2O , as a function of pressure P and temperature T , via the formula:

$$\frac{FLY}{E_d} \Big|_{\lambda}(P, T) = \frac{\chi_{N_2} \cdot \frac{FLY}{E_d} \Big|_{\lambda, P=0}^{N_2}}{1 + P \cdot \tau_{e0} \sum f^i k_e^i(T_0) \sqrt{\frac{T_0}{T}}}, \quad (4)$$

where $\frac{FLY}{E_d} \Big|_{\lambda, P=0}^{N_2}$ is the limit of the FLY ratio for pure nitrogen at $P=0$ hPa (where no quenching effect by molecular collisions is expected) and χ_{N_2} is the mass fraction of nitrogen in the gas admixture ($i = O_2, N_2, H_2O$).

In our model we assume that the fraction of the deposited energy in the gas converted in nitrogen excitation is χ_{N_2} . The parameters entering equation 4: $\frac{FLY}{E_d}|_{\lambda, P=0}^{N_2}$, τ_{e_0} , $k_e^{N_2}(T_0)$, $k_e^{O_2}(T_0)$ and $k_e^{H_2O}(T_0)$ are given for 24 wavelengths (λ) corresponding to 5 excited states (e) at the reference temperature $T_0 = 20^\circ\text{C}$ (293.15 K). The values of these parameters come from both our MACFLY measurements and from already published results: (7) (9) (11) for the spectra (λ) and (12) (13) for the lifetimes (τ_{e_0}) and the quenching factors ($k_e^i(T_0)$).

In this paper, we will show experimental results for pure nitrogen (N_2) and for our experimental dry air (DA) — an admixture 80%(N_2)-20%(O_2) — as a function of the pressure. From this it will be then possible to derive the behavior of the atmospheric dry air (ADA) — an admixture 78.08%(N_2)-0.93%(Ar)-20.99%(O_2) — for which we assume the FLY for argon to be identical to the FLY of nitrogen due to its catalysis effect on nitrogen fluorescence (14). Then the ADA becomes in our model — an admixture 79%(N_2)-21%(O_2).

Using this, we formulate the general FLY of any humid "atmospheric air" (AA), *i.e.* any admixture composed of $(1 - \mu)$ dry air (ADA) and μ water vapor, where μ is the molecular fraction of water in the admixture ($\mu = f^{H_2O}$ as defined in equation 3). We get:

$$\frac{FLY}{E_d}\Big|_{\lambda}^{AA}(P, T, \mu) = \frac{FLY}{E_d}\Big|_{\lambda, P=0}^{ADA} \times \frac{1 - \frac{18}{29}\mu}{1 + P \left(\frac{1-\mu}{P_e^{ADA}(T_0)} + \frac{\mu}{P_e^{H_2O}(T_0)} \right) \sqrt{\frac{T_0}{T}}}, \quad (5)$$

where

$$P_e^{ADA} = \frac{1}{\tau_{e_0} \cdot (0.79k_e^{N_2} + 0.21k_e^{O_2})} \quad \text{and} \quad P_e^{H_2O} = \frac{1}{\tau_{e_0} \cdot k_e^{H_2O}}. \quad (6)$$

We assume that the energy fraction transferred to ADA molecules is proportional to the mass fraction of ADA in the admixture rather than the molecular fraction $(1-\mu)$. The numerator $(1-\frac{18}{29}\mu)$ represents this mass fraction. It is a simplification of the exact formula $\frac{(1-\mu) \cdot 29}{(1-\mu) \cdot 29 + \mu \cdot 18}$ for $\mu \ll 1$ as it is the case in the atmospheric air.

3 Experimental setup

The MACFLY² experiment (15) is twofold, it has been designed to measure both the FLY induced by single electron track and the FLY produced by a high energy electromagnetic shower developing in the air. It is composed of

² Measurement of Air Cherenkov and Fluorescence Light Yield

two devices: MF1 which is used for single track FLY measurements and MF2 which measures the fluorescence produced by an electromagnetic shower. In this paper we will present only the results obtained with MF1 using both a β^- radioactive source (Strontium 90) and an electron test beam (CERN/SPS-X5 line). The results of the shower FLY with MF2 will be presented elsewhere (16).

The MF1 experiment is composed of a pressurized chamber (with pressure from 0 to 1200 hPa) containing the gas, equipped with a trigger system (see Figure 1). This device has an internal cylindrical chamber, 150 mm in diameter and 288 mm long. An ionizing particle ($E \gtrsim 1$ MeV) reaches the gas volume through the entrance window (0.25 mm of black Delrin), crosses the gas volume and leaves the chamber at the exit window (0.8 mm of aluminium) where it reaches the trigger plane.

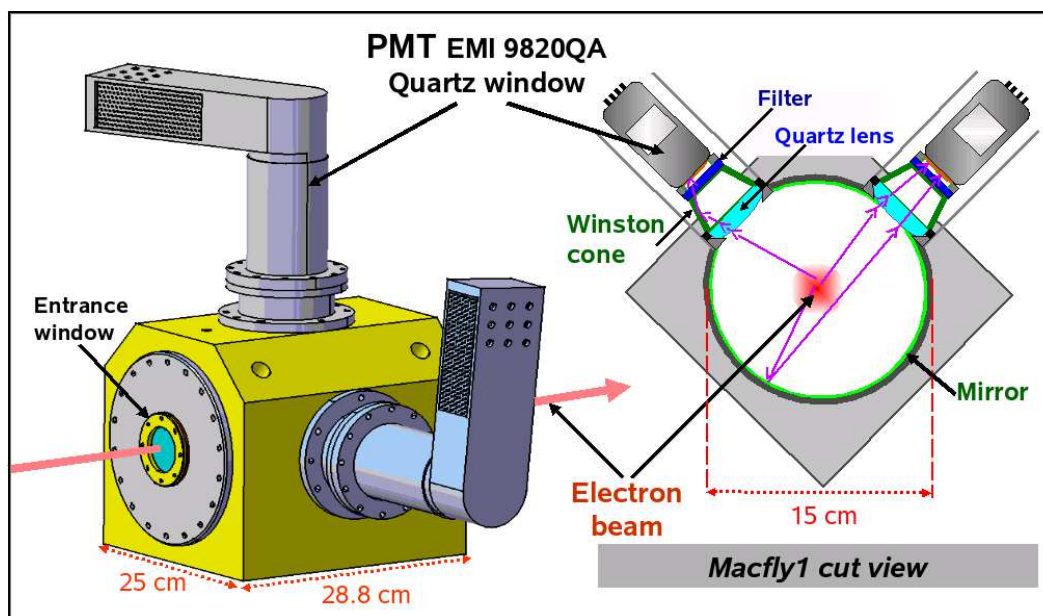


Fig. 1. Schematic view of the MF1 chamber (left) and a cut view of its optical system (right) showing the multilayered mirror, the quartz lens, the Winston cones, the BG3 filters and the PMTs.

An optical system collects the induced fluorescence light, and focuses it on two UV sensitive phototubes (PMT) EMI9820QA. Each PMT receives photons via an optical system which is composed of a multilayered mirror covering the chamber, a quartz lens focusing the light, a Winston cone and wide band filters which allow the selection of the appropriate wavelength. The multilayered mirror³ was designed to have its best reflectance in the appropriate air fluorescence band (see Figure 2). The filters are Schott BG3 filters with a large band of transmittance: 290-440 nm. We have measured the FLY for two gases:

³ From internal to external layer: 90 nm (Al) + 43 nm (SiO_2) + 43 nm (HfO_2) + 43 nm (SiO_2) + 43 nm (HfO_2)

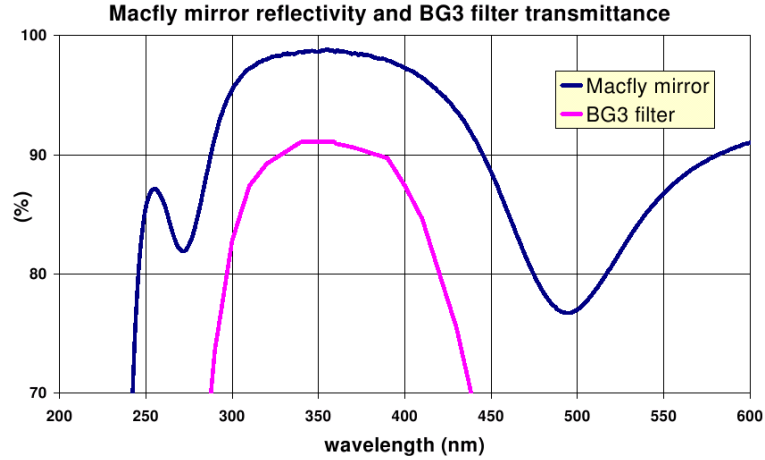


Fig. 2. MF1 multilayered mirror reflectivity coefficient as a function of wavelength (upper curve) and BG3 UV filter transmission coefficient (lower curve).

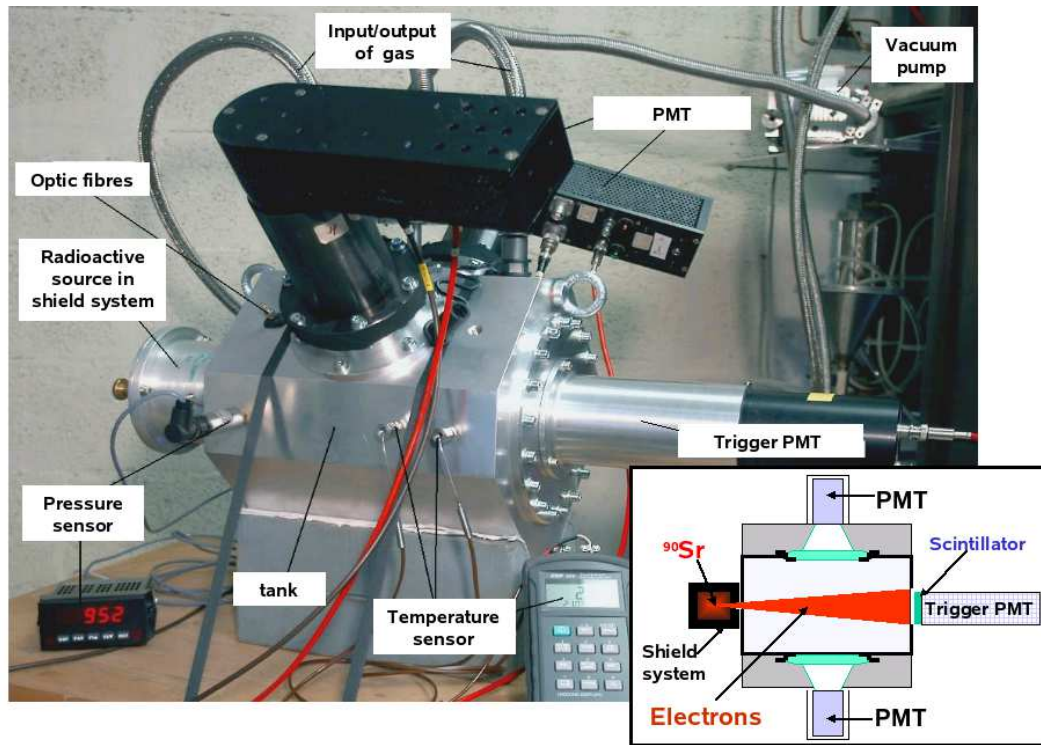


Fig. 3. MF1 setup in its laboratory configuration. The radioactive source is embedded in a shielded box, and the trigger is mounted on the device itself.

pure nitrogen and dry air (N_2 -80%, O_2 -20%). The MF1 experiment was tested in two different setup configurations corresponding to low and high energy. For the low energy runs (labeled MF1-lab) a β^- source (^{90}Sr) was used and the trigger system was integrated in the overall system (see Figure 3). For the high energy runs (labeled MF1-beam) the CERN SPS XP5 beam facility was used. In this later case the source and the trigger system are removed from the main tank, and external systems are installed along the beam line: a position

sensitive ($\sigma \sim 0.5 \text{ mm}$) X-Y delay chamber upstream from the MF1 device to record both the horizontal and the vertical beam position and two double plane trigger systems before and after the MF1 setup. The electron beam was a pulsed beam of about 10 000 electrons per spill (4.8 s duration) every 16.8 s with a beam spot of about $4 \times 7 \text{ mm}^2$. The electron energy was selected in the range between 10 and 100 GeV.

4 Data taking and signal fitting

The data was collected on an event per event basis. For every event the PMT signals (MF1 and trigger counters) were recorded by a QADC (CAEN-V792) which integrated the charge during a gate of 100 ns. The beam position was also recorded for the MF1-beam configuration. During a run, which consists of typically 10^6 triggers, we recorded two kinds of events: the beam events (BE), used for the FLY measurement, and the random events (RE), when no beam is present, for the background estimations and studies. In MF1-lab configuration BE are triggered when an electron reaches the trigger plane after the exit window. In MF1-beam configuration, the electron should reach two trigger planes before and after the MF1 chamber. In the analysis, we also suppressed BE not detected in the central region of the delay chamber.

The FLY is rather weak ($\sim 4 \text{ ph/m}$) and most of the produced photons are lost in the chamber. Among those reaching the PMT photocathode, some are converted in photoelectron (pe). Overall, the mean number of detected photoelectron is about 0.01 pe/event. To extract the mean Detected Light (DL), we performed a fit of the data by a function describing the expected signal; for every event, a PMT detects an integer number of photon: 0, 1, 2 or more converting them into photoelectrons. So the overall PMT spectrum is described by a weighted sum of individual photoelectron contributions, the weights following a Poisson distribution.

The zero photoelectron contribution, the pedestal, is measured experimentally. The single photoelectron contribution is described by two functions: one describing the standard photoelectron multiplication at the first dynode, the other corresponds to the photoelectron being inelastically back-scattered on the first dynode (17). The first function is described by a Weibull⁴ distribution (15) while the second uses an exponential law.

The Multi-photoelectron contributions ($n \geq 2$) are described by gaussian distributions. The mean value μ_n and the variance σ_n^2 of each distribution are determined by the single photoelectron fit function parameters: $\mu_n = n\mu_1 + \mu_0$ and $\sigma_n^2 = n\sigma_1^2$ where μ_1 and σ_1^2 are the single photoelectron distribution (Weibull)

⁴ *Weibull*(x) = $c/b \cdot (x/b)^{c-1} \cdot \exp(-(x/b)^c)$

mean value and variance⁵ and μ_0 the pedestal mean value.

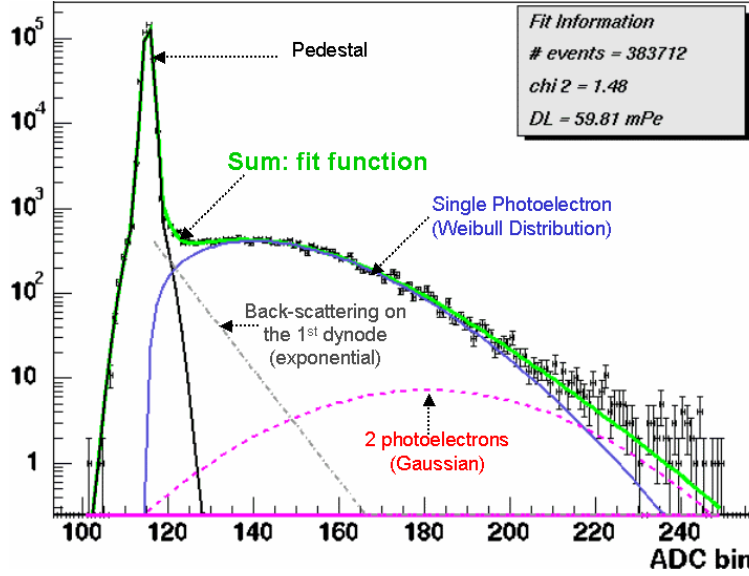


Fig. 4. PMT spectrum fit function (solid line) is a sum of several contributions: pedestal (black solid line), single photoelectron (solid line), multi-photoelectron (dotted line) and back-scattered single photoelectron (dotted dash line).

One can see in Figure 4 the PMT raw signal as well as the different contributions entering the fit function. It is worth noting the agreement between the global fitted function and the data extends on more than five orders of magnitude.

In the context of MACFLY data ($\sim 5 \times 10^5$ BE/run), the low level of PMT dark noise enables the detection of a signal as low as: 0.0002 pe/event, which correspond to a mean sensitivity of the MF1 apparatus of about 0.04 ph/event for the fluorescence light. However other sources of PMT photoelectrons signal degrade this minimal sensitivity to ~ 0.2 ph/event.

The detected light has several origins: fluorescence light (FDL), Cherenkov light (CDL) and background (Bgd).

$$DL = FDL + CDL + Bgd . \quad (7)$$

The Bgd contribution is estimated from both the data from the RE triggers and from BE with vacuum in the chamber (no signal expected).

The Cherenkov contribution is estimated, based on a Geant4 Monte Carlo simulation program, describing in details both the apparatus and the interaction processes (18). For MF1-lab measurements, electrons do not produce any Cherenkov radiation. At high energy ($E > 10$ GeV), the Cherenkov light yield is important but its contribution to the raw PMT signal remains small;

⁵ $\mu_1 = b \cdot \Gamma(1 + \frac{1}{c})$ and $\sigma_1 = b \sqrt{\Gamma(1 + \frac{2}{c}) - (\Gamma(1 + \frac{1}{c}))^2}$

the Cherenkov light is emitted in the forward direction where a black "light catcher" is installed, suppressing dramatically the reflected Cherenkov component.

Figure 5 shows the DL measured and the estimation of CDL and Bgd for test beam measurements at CERN as a function of pressure in Dry Air and nitrogen. The FDL is determined by subtraction. We can see that the main part of the DL comes from the fluorescence. The Fluorescence Light Yield in

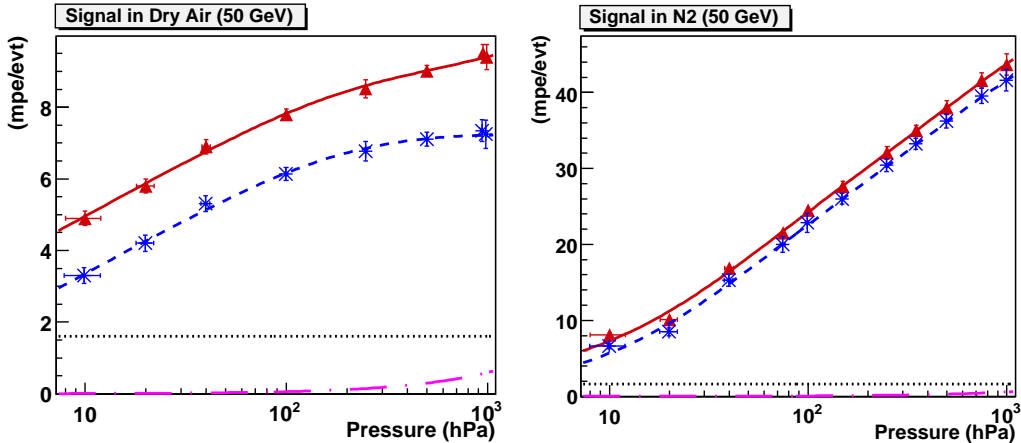


Fig. 5. Measured light in dry air (left) and in pure nitrogen (right) in milli-photoelectron per event (mpe/evt) as a function of the gas pressure. Triangles are raw measured light data (DL); dotted line is the Bgd estimation from vacuum measurements; dotted dash line is CDL simulation; stars are the FDL data (after subtraction of Bgd and CDL); dashed line is a simple FLY model fit and the solid line is its projection on DL.

MF1, is determined from the measurements from both overall and background signals and from the estimated contribution for the Cherenkov yield:

$$FLY = \frac{DL - CDL - Bgd}{\varepsilon_{MF1}}, \quad (8)$$

where the MF1 efficiency ε_{MF1} is the product of geometrical acceptance of the detector and of the PMT quantum efficiency ($\varepsilon_{MF1-beam} = 0.00556 \text{ ph/pe}$).

5 Calibration and systematics

The geometrical acceptance is estimated by a Geant4 (18) simulation program which describes in detail the apparatus. It is able to perform the tracking of the optical photons from the production source along the electron track to the PMT photocathodes (Filters transmittance and Mirror reflectivity are included). The simulation result shows that 2.75% of the fluorescence light emitted isotropically in the chamber reaches one PMT photocathode.

Uncertainty sources	MF1-lab	MF1-beam
Electron position	5%	6%
Mirror	4%	4%
Winston cone	2%	2%
Row aluminum	3%	3%
Cherenkov catcher	0%	1%
Others (lens, filter ...)	< 2 %	< 2%
Geometrical Acceptance	7.5%	8.2%

Table 1

Geometrical acceptance systematic uncertainties for both experimental configurations : MF1-lab (with ^{90}Sr source) and MF1-beam (CERN test beam)

This geometrical acceptance varies with the setup configuration (mirror, surfaces, filters,...). The optical properties of the inner surfaces are well known: the mirror reflectance, as function of wavelength, was measured with less than 2% of error. Figure 2 shows the result of this measurement. The other inner surfaces were studied in laboratory with a calibration device at 370 nm.

To check our Geant4 based simulation program, we compared the FLY measurements for different experimental (optical system) configurations with the simulation expectations. For instance, having black covered some inner surfaces, the geometrical acceptance was reduced by 24% which was really close to the predicted simulation value of 26%.

Table 1 summarizes the systematic relative errors on geometrical acceptance for both experimental configurations (MF1-lab and MF1-beam). The main contributions come from the electron track position uncertainty (delay chamber/MF1 alignment and multiple-scattering in the chamber), from the internal surfaces reflective properties and from the mirror inhomogeneity. The overall geometrical acceptance uncertainty is estimated to 7.5% for MF1-lab and 8.2% for MF1-beam.

The others sources of systematic uncertainty come from our reconstruction method used to extract the fluorescence signal from the data and from the PMT calibration. We identified three sources of errors from our reconstruction method: PMT signal fitting procedure (DL reconstruction error), background and Cherenkov estimations. These uncertainties vary with the setup configuration and depend on the signal intensity.

Table 2 gives our estimation of the systematics uncertainty for dry air measurements with the MF1 setup for both laboratory and test beam configurations. The total absolute uncertainty is 13.2% for MF1-lab and 13.7% for MF1-beam. They are dominated by PMT calibration uncertainties.

Errors sources	MF1-lab	MF1-beam
Geometrical Acceptance	7.5%	8.2%
PMT calibration	10%	10%
DL reconstruction	4%	3.5%
CDL Simulation	0%	2%
Bgd Measurement	1%	2%
Systematic Error	13.2%	13.7%

Table 2

Systematic uncertainties on the FLY measurement for both experimental configurations: MF1-lab and MF1-beam.

6 Results

In our air FLY model presented in section 2, the light yield is proportional to the deposited energy in air (E_d). Therefore the ratio $\frac{FLY}{E_d}$ becomes independent of the energy lost by the incoming electron. It will only vary as a function of the atmospheric conditions (pressure, temperature and humidity).

In the data used for this paper, the pressure is the only parameter under consideration. Figure 6 shows the $\frac{FLY}{E_d}$ measured by MF1, in the wavelength range 290-440 nm, as a function of the pressure, both in our experimental dry air (DA) and in pure nitrogen for different energies of the incoming electron: 1.5 MeV, 20 and 50 GeV. The dotted lines correspond to our FLY model described in section 2 (equation 4), fitted on the MACFLY data, for which $i = N_2, O_2$. We have fitted the absolute value and the pressure dependence of the FLY (from 3 hPa to 1100 hPa) both in our dry air (DA) and in pure nitrogen (in same time). The fit had 3 free parameters: the 290-440 nm integral value of pure nitrogen FLY and the mean value of the $k_e^{N_2}$ and of the $k_e^{O_2}$.

The zero pressure extrapolation FLY obtained, respectively, for pure nitrogen and dry air are:

$$\left. \frac{FLY}{E_d} \right|_{P=0}^{N_2} = 1959 \pm 412 \text{ ph/MeV} \quad \text{and} \quad \left. \frac{FLY}{E_d} \right|_{P=0}^{DA} = 1523 \pm 329 \text{ ph/MeV} .$$

The first integral value is used to compute the $\frac{FLY}{E_d} \Big|_{\lambda, P=0}^{N_2}$ values for the 24 λ , according to the spectral published values (7) (9) (11). In the same way, the two mean k_e^i values extracted from our pressure dependence measurements are used to compute the 10 k_e^i for the five exited states according the relative values from (12) (13). Table 3 summarizes the values of all the parameters used in our model. The P' are determined by the equation 6 with the fitted k_e^i and already published life times (12) (13).

At atmospheric pressure and $T = 23^\circ\text{C}$ in dry atmospheric air, our FLY model

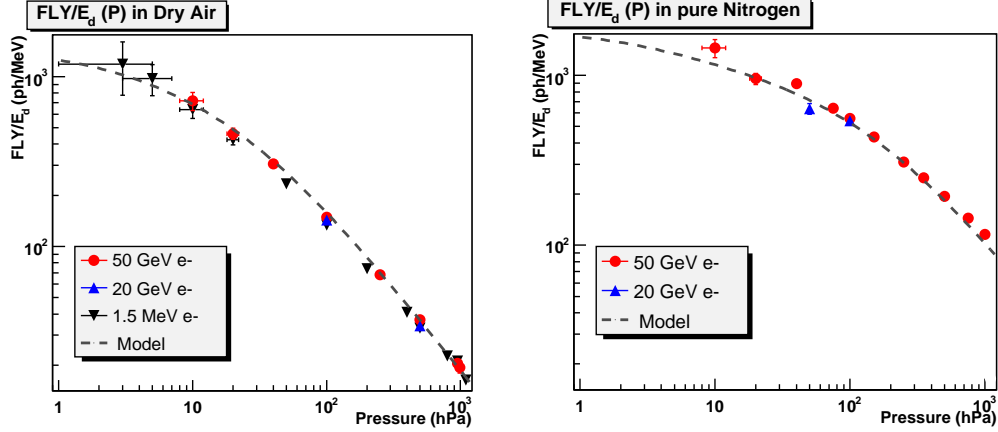


Fig. 6. Ratio FLY/E_d - "FLY on deposited Energy" as a function of the pressure, in our experimental dry air — DA — (left) and in pure nitrogen — N_2 — (right), measured for different electron energies: 1.5 MeV (\blacktriangledown), 20 GeV (\blacktriangle) and 50 GeV (\bullet). The dotted lines show the results of the fit of the data by our FLY model.

fitted on MACFLY data gives:

$$\left. \frac{FLY}{E_d} \right|^{ADA} = 17.6 \pm 2.3 \text{ ph/MeV} . \quad (9)$$

The ratio of the FLY/E_d for pure nitrogen compared with the one for dry air, is shown in figure 7 as a function of the pressure.

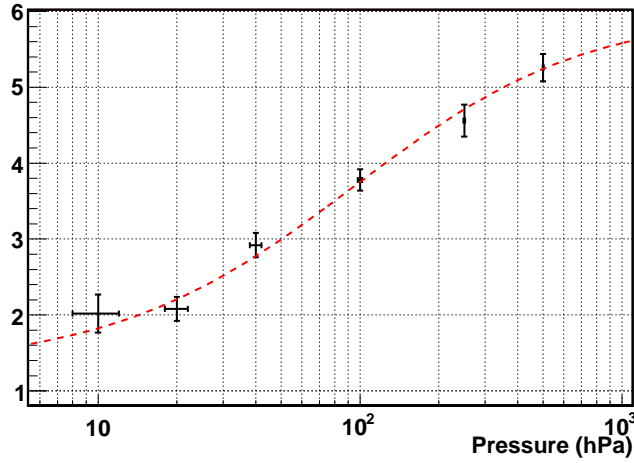


Fig. 7. Ratio of the FLY/E_d in N_2 and in dry air as function of pressure. The dotted line is the fluorescence model fit on MF1 data

At zero pressure this ratio tends to the ratio of nitrogen mass fraction in each gas ($1/\chi_{N_2}^{DA} = 1.286$), while at atmospheric pressure the quenching effect of the oxygen reduces by about a factor 5.5 the FLY in pure nitrogen.

During the data taking we measured the FLY from a "real" humid atmospheric air (RAA). We filled MF1 chamber with the ambient laboratory air having the

Excited state	λ (nm)	MACFLY Model Parameters					Atmospheric air		
		$\frac{FLY}{E_d} _{\lambda, P=0}^{N_2}$ (ph/MeV)	τ_{e_0} (ns)	$k_{e(20^\circ C)}^{N_2}$ (ms ⁻¹ .Pa ⁻¹)	$k_{e(20^\circ C)}^{O_2}$ (ms ⁻¹ .Pa ⁻¹)	$k_{e(20^\circ C)}^{H_2O}$ (ms ⁻¹ .Pa ⁻¹)	$\frac{FLY}{E_d} _{\lambda, P=0}^{ADA}$ (ph/MeV)	$P_{e(20^\circ C)}^{ADA}$ (hPa)	$P'_{e(20^\circ C)}^{H_2O}$ (hPa)
$C^3\Pi_u$ $\nu=0$	337.1	227	37	1.65	43.6	92	174	25.8	2.94
	357.7	182					139		
	380.5	64					49		
	405.9	26					20		
	434.4	7					5		
$C^3\Pi_u$ $\nu=1$	315.9	149	40	4.18	54.0	95	114	17.1	2.63
	333.9	7					5		
	353.7	48					37		
	375.6	63					49		
	399.8	39					30		
	427.0	10					8		
$C^3\Pi_u$ $\nu=2$	297.7	31	40	7.35	77.0	98	24	11.4	2.55
	313.6	52					40		
	350.0	7					6		
	371.1	23					18		
	394.3	16					13		
	420.1	11					8		
$C^3\Pi_u$ $\nu=3$	296.2	20	40	9.06	113	111	15	8.8	2.25
	328.5	34					26		
	346.9	9					7		
	367.2	8					6		
	389.4	5					4		
$B^2\Sigma_u^+$ $\nu=0$	391.4	662	62	38.7	96.8	211	508	3.17	0.76
	427.8	259					198		

Table 3

Parameters used in our MACFLY model describing both a general N_2, O_2, H_2O admixture as defined in equation 4 and its simplification for an atmospheric air (equation 5). The 24 wavelengths (grouped per excited states) and the excited states enter the first two columns. The other columns contain the values of the parameters. Among them the bolded ones are obtained by fitting the MACFLY data.

Energy	FLY/E_d (ph/MeV)	FLY/l (ph/m)
1.5 MeV	17.0±2.3	3.14±0.41
20 GeV	17.4±2.5	4.22±0.61
50 GeV	18.2±2.5	4.44±0.61
All energies	17.6±2.3	

Table 4

Values of the FLY (FLY/E_d and FLY/l) for the 3 energy samples, at the reference point ($P=1013$ hPa, $T = 23^\circ C$, $\mu=0$) for atmospheric dry air (ADA). The last line shows the value of FLY/E_d when all the data are fitted together.

following parameters: $P=950$ hPa, $T = 23^\circ C$ and relative humidity 35% (informations provided by external probes). This corresponds to an atmospheric air (AA) with a water vapor fraction $\mu = 1.05\%$. We compared this measurement with a result from our Dry Air at same pressure and temperature. We found:

$$\frac{FLY^{DA}}{FLY^{RAA}} = 1.11 \pm 0.07, \quad (10)$$

while the expected value from our model is 1.13.

7 Comparison with other experiments

To compare our results with the other experiments, we have chosen a reference point: atmospheric dry air at $P=1013$ hPa (1 atm.) and $T = 23^\circ\text{C}$ (296 K), and we express the FLY per track length (FLY/l) in the usual units: photon per track length (ph/m). Table 4 gives values we obtained for three electron energies: 1.5 MeV, 20 GeV and 50 GeV. These values are corrected, according to our fluorescence model, to correspond to this reference point.

In Figure 8 we show the FLY/l measurements of the corrected MACFLY data together with the values for others experiments as a function of the incoming kinetic energy. On the same figure we show the expected energy depositions in the gas. The experimental data come from the following experiments: former results of Nagano et al. (for 0.85 MeV electrons), the results of Kakimoto et al., at 1.4 MeV, 300 MeV, 650 MeV and 1000 MeV, and the recent results of the FLASH experiment (19) for 28.5 GeV electrons.

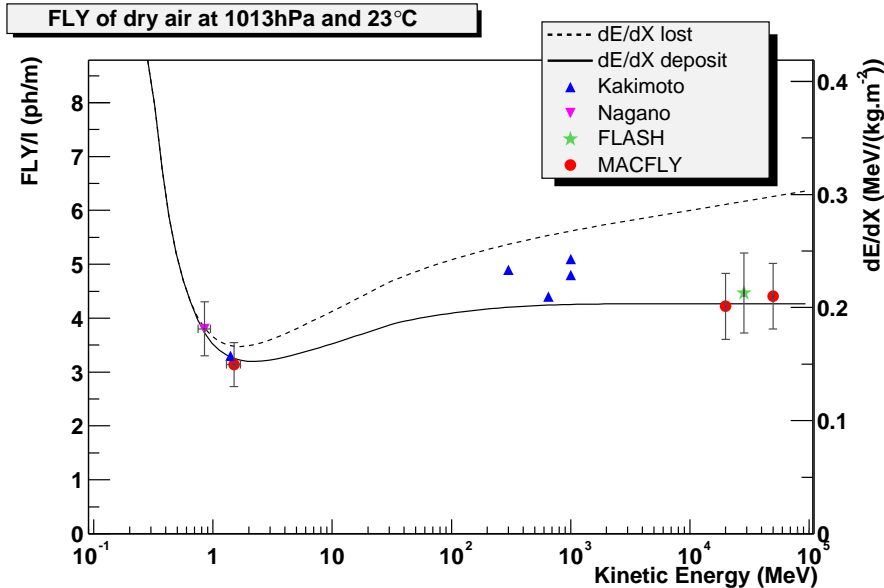


Fig. 8. FLY per electron track length FLY/l (in photon/meter) as a function of electron energy measured by several experiments (see text). We also show the energy depositions (right axis): energy lost dE/dX (dashed curve) and the energy deposited dE_d/dX in MF1 chamber (solid curve).

The variation of FLY/l (left axis of figure 8) as a function of the electron energy is compared to the dE/dX of the electron (right axis). The beam electrons lose their energy by ionization and by producing high energy delta and gamma rays. The dotted line shows the total dE/dX lost by the an electron, calculated using Berger-Seltzer formula (20) which is used by Geant4 simulation toolkit (18). The solid line indicates the energy deposited (dE_d/dX) in the fiducial gas volume of the MF1 chamber, computed with our MF1 simulation

program (15). The difference between the two curves dE/dX and dE_d/dX reflects the energy carried away by the high energy δ -rays and γ -rays beyond the MF1 chamber. The ratio between the two scales corresponds to our FLY model at this reference point: $FLY/E_d = 17.6 \text{ ph/MeV}$.

On a wide energy range (from MeV region to 50 GeV region) the MACFLY data are well described by the deposited energy distribution. At low energy our measurement is in agreement with results from Nagano et al. and Kakimoto et al., following the Berger-Seltzer curve. At high energy they also agree well with the FLASH result, showing the deposited energy behaviour of the FLY.

8 Conclusions

We have performed measurements of the dry air and pure nitrogen Fluorescence Light Yields induced by single electrons of low (1.5 MeV) and high (20 and 50 GeV) energy as a function of the gas pressure. We show that, within the experimental uncertainties, the FLY is proportional to the deposited energy in the gas, independently of the incoming electron energy. At the reference point: $P=1013 \text{ hPa}$ and $T = 20^\circ\text{C}$, the $FLY/E_d = 17.6 \pm 2.3 \text{ ph/MeV}$.

Based on our measurements and using already published data we have proposed a model describing, in the 390-440 nm range, the fluorescence light yield for any air composition, as a function of the pressure, the temperature and the water contamination.

9 Acknowledgments

This work has been partly supported by a fund from the Institut National de Physique Nucléaire et de Physique des Particules and from the Joint Institute for Nuclear Research. We would like to thank the Centre Européen de Recherche Nucléaire who allocated two weeks of beam test on the SPS beam line and particularly the CERN PH-DT2 (Detector Technology) group. Many thanks to our colleagues from the Alice experiment who helped and supported our activity in the test beam area and to M. Maire for his Geant4 expertise.

References

- [1] K. Greisen, *Phys. Rev. Lett.* **16** 748 (1966) ;
V. A. Kuzmin, G. T. Zatsepin, *Pisma Zh. Eksp. Teor. Fiz.* **4** 114 (1966).

- [2] M. Takeda *et al.*, *Astro. J.* **522**, 255 (1999).
- [3] R.U. Abbasi *et al.*, *Phys. Rev. Lett.* **92**, 151101 (2004).
- [4] J. Abraham *et al.*(AUGER coll.), *Nucl. Instrum. Meth. A* **523**, 50 (2004).
- [5] G.B. Thomson and the TA/TALE coll., *29th International Cosmic Ray Conferences (ICRC 2005), Pune, India*, Vol. **8**, 363. (2005)
- [6] J. Linsley (OWL project), *26th International Cosmic Ray Conference (ICRC 1999), Salt Lake City, USA*, Proceedings Vol. **2**, 423. (1999);
O. Catalano and A. Petrolini (EUSO coll.), *29th International Cosmic Ray Conferences (ICRC 2005), Pune, India*, Vol. **8**, 93. (2005);
L. Tkatchev *et al.* (TUS coll.), *29th International Cosmic Ray Conferences (ICRC 2005), Pune, India* Vol **8**, 263. (2005)
- [7] A. N. Bunner, "Cosmic Ray Detection by Atmospheric Fluorescence" Ph. D. thesis (Cornell University) (1967).
- [8] F. Kakimoto *et al.*, *Nucl. Instrum. Meth.*, **A 372** 527 (1996).
- [9] M. Nagano *et al.*, *Astropart. Phys.* **22** 235(2004).
- [10] P. Nedelec and P. Colin, "Air Fluorescence Light Yield Measurements" proceeding of the 40th "Rencontres de Moriond", La Thuile, (2005).
<http://moriond.in2p3.fr/J05/>
- [11] G. Davidson and R O'Neil, *J. of Chem. Phys.* **41** 12 3946 (1964).
- [12] S.V. Pancheshnyi *et al.*, *Chem. Phys. Lett* **294** 6 523 (1998);
S.V. Pancheshnyi *et al.*, *Chem. Phys.* **262** 349-357 (2000).
- [13] H. Brunet, Ph. D. thesis, University P. Sabatier, Toulouse (1973).
- [14] A. E. Grun and E. Schopper, *Z. Naturforsch.* **9a**. 134 (1954).
- [15] P. Colin, "Reconstruction des gerbes atmosphériques et mesure de la fluorescence de l'air...", Ph. D. thesis (University Joseph Fourier, Grenoble) LAPP-T-2005-06 (2005).
<http://lappweb.in2p3.fr/MACFLY/>
- [16] P. Colin *et al.*, (MACFLY collaboration), "Measurement of air fluorescence light yield induced by electromagnetic air showers", in preparation for *Astropart. Phys.*
- [17] Philips Photonics, "Photomultiplier tubes, principle & application", Philips Export B.V. (1994).
- [18] H. P. Weillish., M. Maire and L. Urban "Geant4 Physics reference manual", (2004).
<http://geant4.web.cern.ch/geant4/>
- [19] J. W. Belz *et al.*, *Astropart. Phys.* **25** 129 (2006).
- [20] S. M. Seltzer and M. J. Berger, *Int. J. Appl. Radiat. Isot.* **33** 1189 (1982);
R. M. Sternheimer, M. J. Berger and S. M. Seltzer, *Atomic Data and Nuclear Data Tables* **30** 261 (1984).

List of Figures

- 1 Schematic view of the MF1 chamber (left) and a cut view of its optical system (right) showing the multilayered mirror, the quartz lens, the Winston cones, the BG3 filters and the PMTs. 6
- 2 MF1 multilayered mirror reflectivity coefficient as a function of wavelength (upper curve) and BG3 UV filter transmission coefficient (lower curve). 7
- 3 MF1 setup in its laboratory configuration. The radioactive source is embedded in a shielded box, and the trigger is mounted on the device itself. 7
- 4 PMT spectrum fit function (solid line) is a sum of several contributions: pedestal (black solid line), single photoelectron (solid line), multi-photoelectron (dotted line) and back-scattered single photoelectron (dotted dash line). 9
- 5 Measured light in dry air (left) and in pure nitrogen (right) in milli-photoelectron per event (mpe/evt) as a function of the gas pressure. Triangles are raw measured light data (DL); dotted line is the Bgd estimation from vacuum measurements; dotted dash line is CDL simulation; stars are the FDL data (after subtraction of Bgd and CDL); dashed line is a simple FLY model fit and the solid line is its projection on DL. 10
- 6 Ratio FLY/E_d - "FLY on deposited Energy" as a function of the pressure, in our experimental dry air — DA — (left) and in pure nitrogen — N_2 — (right), measured for different electron energies: 1.5 MeV (\blacktriangledown), 20 GeV (\blacktriangle) and 50 GeV(\bullet). The dotted lines show the results of the fit of the data by our FLY model. 13
- 7 Ratio of the FLY/E_d in N_2 and in dry air as function of pressure. The dotted line is the fluorescence model fit on MF1 data 13
- 8 FLY per electron track length FLY/l (in photon/meter) as a function of electron energy measured by several experiments (see text). We also show the energy depositions (right axis): energy lost dE/dX (dashed curve) and the energy deposited dE_d/dX in MF1 chamber (solid curve). 15

List of Tables

- 1 Geometrical acceptance systematic uncertainties for both experimental configurations : MF1-lab (with ^{90}Sr source) and MF1-beam (CERN test beam) 11
- 2 Systematic uncertainties on the FLY measurement for both experimental configurations: MF1-lab and MF1-beam. 12
- 3 Parameters used in our MACFLY model describing both a general N_2, O_2, H_2O admixture as defined in equation 4 and its simplification for an atmospheric air (equation 5). The 24 wavelengths (grouped per excited states) and the excited states enter the first two columns. The other columns contain the values of the parameters. Among them the bolded ones are obtained by fitting the MACFLY data. 14
- 4 Values of the FLY (FLY/E_d and FLY/l) for the 3 energy samples, at the reference point ($P=1013$ hPa, $T = 23^\circ\text{C}$, $\mu=0$) for atmospheric dry air (ADA). The last line shows the value of FLY/E_d when all the data are fitted together. 14